

Anisotropic Vortex Lattice in $\text{YBa}_2\text{Cu}_3\text{O}_7$ M. Yethiraj,¹ H. A. Mook,¹ G. D. Wignall,¹ R. Cubitt,² E. M. Forgan,² S. L. Lee,³ D. M. Paul,⁴ and T. Armstrong⁵¹*Solid State Division, Oak Ridge National Laboratory, Oak Ridge, Tennessee 37831-6393*²*Superconductivity Research Group, University of Birmingham, Birmingham B15 2TT, United Kingdom*³*Physik-Institut der Universität Zürich, Schönberggasse 9, CH 8001, Zürich, Switzerland*⁴*Department of Physics, University of Warwick, Coventry CV4 7AL, United Kingdom*⁵*Allied Signal Research Laboratories, Torrance, California 90509*

(Received 3 May 1993)

We report on small angle neutron scattering observations of the flux line lattice (FLL) in a single crystal of $\text{YBa}_2\text{Cu}_3\text{O}_7$. To probe the mass anisotropy ratio, m_3/m_1 , measurements were made as a function of angle, Θ , between the 8 kOe applied field and the crystallographic (001) axis for $0^\circ \leq \Theta \leq 80^\circ$. With the rotation about an a/b (or y) axis, two symmetry-related distorted hexagonal FLL domains formed. Contrary to theoretical prediction, the lattices formed are consistent with a rotation of the short basis vector, \mathbf{a}_1 , from the x axis by 15° , after the effects of anisotropy are removed. The mass ratio is 20 ± 2 , which is slightly lower than published values. The temperature dependence of the intensity is not conventional.

PACS numbers: 74.72.Bk, 74.60.Ge

The high T_c superconductors are highly anisotropic. In general, these compounds are nominally uniaxial systems since the a - b (basal plane) anisotropy is fairly small and the c axis is considerably different. In $\text{YBa}_2\text{Cu}_3\text{O}_7$, the crystal structure is nearly tetragonal with $c \approx 3a$ and the a/b ratio is approximately 0.99. There has been much discussion about the role this anisotropy plays in superconductivity in these materials. Clearly, information regarding the behavior of vortex lattices in low symmetry geometries is extremely important.

This is the first study of the anisotropy in YBCO that measures the vortex lattice in a bulk sample directly. Small-angle neutron scattering studies yield information about the structure of the lattice that can be used to determine accurately the anisotropy ratio, γ . A difference in γ is seen directly in the ratio of lengths of the basis vectors of the lattice and the uncertainty is substantially smaller by this technique than many other methods. For example, the difference between $\gamma=5$ and $\gamma=8$ that were obtained in two different measurements [1,2] would be painfully obvious in small-angle neutron scattering (SANS) measurements. Although the same is true of decoration methods, the fields used in those experiments are extremely small and often smaller than the lower critical field, H_{c1} , at the lowest temperatures, hence what is observed is a reflection of flux trapped close to T_c . Our results were obtained at fields substantially larger than H_{c1} .

We have previously reported [3] on the properties of the flux line lattice in $\text{YBa}_2\text{Cu}_3\text{O}_7$ with the applied field along the c axis and for the case where the field was 30° from the c axis. These studies have been extended in order to probe the mass anisotropy ratio, m_3/m_1 , and measurements were made as a function of angle, Θ , between the 8 kOe applied field and the crystallographic (001) axis at a series of angles with $0^\circ \leq \Theta \leq 80^\circ$. (Note: m_3

and m_1 are the effective masses of the electron in the basal plane and along the c axis, respectively.)

The 7.8 g sample of $\text{YBa}_2\text{Cu}_3\text{O}_7$ is the same as used previously (mosaic $\approx 0.6^\circ$) and the experimental setup was much the same. The sample was cooled in a closed-cycle helium refrigerator and was mounted between the coils of an electromagnet. The lowest sample temperature was 11 K with a stability of ± 0.1 K (absolute accuracy ± 0.5 K). The applied field was 8 kOe. The c axis of the sample and the field direction were aligned *in situ* such that they initially coincided with the incident neutron direction.

In this experiment, the sample was mounted such that an a/b axis of the crystal was vertical. Note that since our sample is twinned, a single direction represents a random mix of both the (100) and the (010) directions. Rotations of the c axis away from the field direction were performed about this (100)/(010) axis. This sets up a clean geometry (Fig. 1) to study the crystallography of the flux lattice and also minimizes the effect on the flux line lattice (FLL) of the twin planes, which are along the $\{110\}$ directions. When c was rotated away from B , the flux lines were no longer parallel to the twin planes.

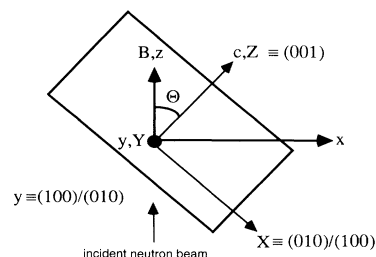


FIG. 1. A schematic of the experimental geometry, viewed along the axis of rotation of the sample.

When the applied field (B) was along the c axis a diffraction pattern with square symmetry was seen. As has been previously reported, this is due to two sets of orthogonal 1D arrangements corresponding to the $\{110\}$ twin plane directions. The basal plane is nearly isotropic and further, the a - b twinning in the crystal makes any basal plane flux lattice anisotropy impossible to measure. It is anticipated that a hexagonal lattice would form in untwinned crystals. As the angle (Θ) between the applied field, B , and c is increased, the c - ab anisotropy becomes evident. In this case, the field distribution of an isolated flux line no longer has a circular cross section since the London penetration depths in the two directions are different. A distorted hexagonal lattice results. The data were taken with the field and the flux lines aligned along the beam. Hence, none of the spots were exactly on the Bragg condition, which would have the neutron beam at the Bragg angle to a flux lattice plane. Clearly, it is impossible to have all reflections at the Bragg angle simultaneously. The large observed mosaic of the FLL meant that, in our arrangement, all spots could be observed simultaneously without severe loss of intensity. However, due to the small instrumental ($< 5\%$) $\delta\lambda/\lambda$ of the SANS instrument at high-flux isotope reactor (HFIR) in addition to the large FLL mosaic, the calculated movement of the diffracted beam position due to (flux) crystal misalignment is small and appropriate corrections [4] can be made. When B was exactly along the a axis ($\Theta=90^\circ$), strong metallurgical scattering obliterated any FLL signal that might have been observed. As has been noted previously, this strongly angle-dependent scattering has been used to check the crystal alignment of our samples.

When B was at an angle, Θ , to the c axis, twelve distinct diffraction spots were observed, shown in Fig. 2 for $\Theta=(a)$ 45° , (b) 60° , and (c) 70° from the c axis. (Note that peaks on the right hand side are closer to being on the Bragg condition and hence are more intense. Also, a peak on one side implies that the same planes will give rise to the second peak on the opposite side, with an appropriate rotation to bring it into Bragg diffracting condition.) The twelve peaks observed are due to two symmetry-related domains of the distorted hexagonal lattice. The two domains were rotated away from the vertical y axis in opposite directions from each other. The angle of rotation varied with Θ in a manner consistent with $\alpha=15^\circ$. Here, α is the angle between the basis vector and the x axis in a lattice undistorted by anisotropy. The actual angle, β , between a_1 and x when the effects of the anisotropy is included varies with the effective degree of anisotropy, which in turn increases with Θ and is given by

$$\tan\beta = \left(\frac{m_3}{m_{zz}} \right)^{1/2} \tan\alpha,$$

$$\frac{m_{zz}}{m_3} = \cos^2\Theta + \gamma^{-2} \sin^2\Theta, \quad \gamma^2 = \frac{m_3}{m_1}.$$

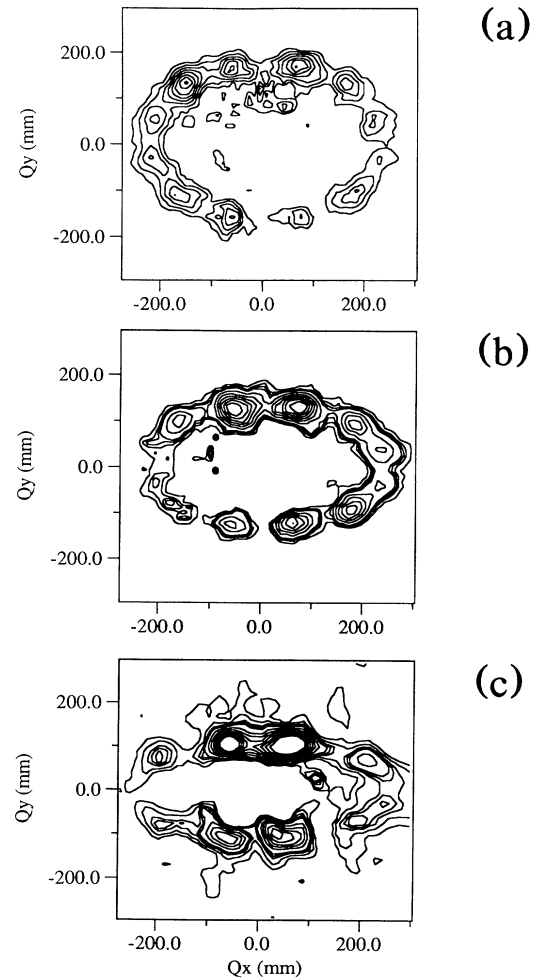


FIG. 2. A contour plot of the diffracted intensity for the applied field (a) 45° , (b) 60° , and (c) 70° from the c axis. Slight misalignments between field direction and neutron beam direction manifest themselves as intensity variations, e.g., between top left and bottom right of (a). The applied field was 8 kOe for the 45° and 60° cases; the applied field used for the 70° data was 5 kOe in order to see all the peaks while maintaining the same instrumental resolution. The source aperture was 12 mm in diameter, which was 7 m from the sample. The aperture at the sample was 6 mm in diameter. The sample-detector distance was 19.7 m.

(The usage of α and Θ here is the same as in Ref. [5]. Note: $\alpha=15^\circ$ is identical to $\alpha=45^\circ$ or 75° since in each case the unit cell that results is identical.) Like many other systems [5,6], this is clearly different from what is predicted from theoretical considerations [7] of a weak interaction favoring $\alpha=0$. The basis vectors of the flux line lattice, \mathbf{a}_1 and \mathbf{a}_2 , and the unit cell are indicated (for $\Theta=60^\circ$) in Fig. 3(a). Figure 3(b) shows the resulting reciprocal lattice. The basis vectors of the symmetry-related domain can be generated by a simple mirror ($X \rightarrow -X$) or ($Y \rightarrow -Y$) transformation.

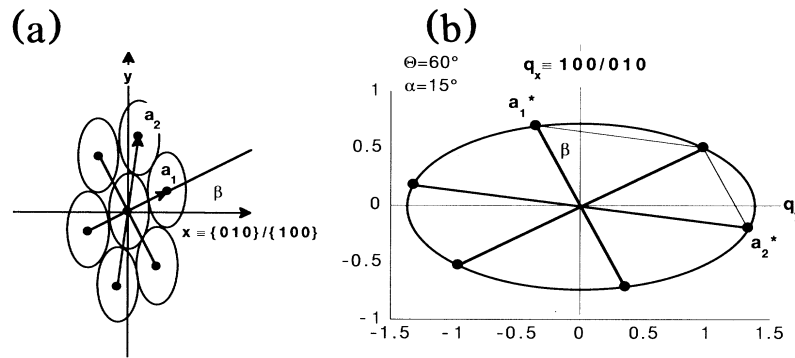


FIG. 3. (a) The real space arrangement of the flux lines for one of the lattices corresponding to $\Theta=60^\circ$ and $\alpha=15^\circ$ (see text for details). (b) The reciprocal lattice derived from the real space configuration shown in (a).

These preferred orientations of the FLL may arise from an interaction between the flux lines and the crystal symmetry. However, they may also indicate a residual pinning effect of the twin planes. If we suppose that the flux lattice planes are oriented such that they tend to include intersections of twin planes and CuO_2 planes, the resulting FLL orientation is indistinguishable from the $\alpha=15^\circ$ case for $\Theta \leq 70^\circ$. In our present $\Theta=80^\circ$ data, we cannot accurately determine the exact lattice structure. However, the fact that pinning at the planes is more energetically favorable does not imply pancakes vortices. For the degree of anisotropy observed, the flux lines should still be three dimensional. Note that pinning effects of twin planes have been observed by other techniques [8,9] for $\Theta \neq 0^\circ$, although these measurements are at rather different fields than employed here.

In previous measurements with B 30° from the c axis, a sixfold pattern was observed and the tangential angular spread was much larger than the instrumental resolution. The difference in the present measurements is that the rotation was about the 100 axis, whereas in the previous experiment the rotation was about an axis $\sim 22^\circ$ from the 110. It is possible that, in the sixfold pattern seen before, the large observed tangential angular spread is in fact due to two distinct sets of resolution-limited sixfolds spots.

The rocking curve of the FLL for $\Theta=45^\circ$ had a mosaic of $\sim 1^\circ$, compared to $\sim 2^\circ$ obtained with $B \parallel c$ at the same field. In addition, the FWHM $\delta d/d$ of this lattice was smaller ($12\% \pm 7\%$) than that of the "square lattice." Both of the above indicate a more perfect lattice for the anisotropic case. The increased perfection of the lattice is probably due to the reduced influence of twin plane pinning. (Note: The mosaic of the flux line lattice at $\Theta=45^\circ$ is slightly larger than the crystalline mosaic of the sample, which is approximately 0.6° .)

Irrespective of the actual crystallography of the lattice, all diffracted spots can be shown to fall on an ellipse whose axial ratio is given by $\sqrt{m_{zz}/m_3}$. This measure is independent of the structure details. Further, in the experiment, the axial ratio of the ellipse is more accurately

measured than the a_1/a_2 ratio or the angle between a_1 and a_2 , which can also be used to deduce γ^2 . The position of the Bragg peak is changed slightly by not positioning the flux line crystal on the Bragg condition. The positional shift is small ($\approx 2\%$ for $\Theta=70^\circ$) in absolute terms and the effect of the "misalignment" is even smaller when the axial ratio of the ellipse is considered since both x and y axes are affected. Corrections for this positional shift have been made. The square of the (corrected) ratio of the minor to major axis of the ellipse is plotted against $\sin^2\Theta$ in Fig. 4. The data were fitted to a straight line which gave a slope of -0.9503 ± 0.003 . The value of the γ^2 obtained from the axial ratio of the ellipse as a function of Θ is 20 ± 2 ($\gamma=4.6 \pm 0.2$). Values of γ^2 in the literature are rather variable, with the most common value being approximately 25. However, it should be noted that some of these variations may be due to varying oxygen content [10]. The crystal mosaic will also tend to reduce the value of γ somewhat, although this effect is small (and smaller than our estimated uncertainty) in our relatively perfect crystal. Our low γ value represents a

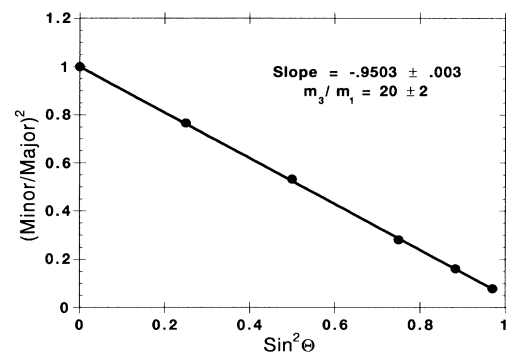


FIG. 4. The axial ratio is plotted as a function of $\sin^2\Theta$, where Θ is the angle between the field and the c axis. The mass anisotropy ratio, γ^2 , can be determined by the ratio of the minor to major axis of the ellipse on which the scattered intensity falls. The square of the axial ratio is proportional to $\cos^2\Theta + \gamma^{-2}\sin^2\Theta$. γ obtained from the slope is 20 ± 2 .

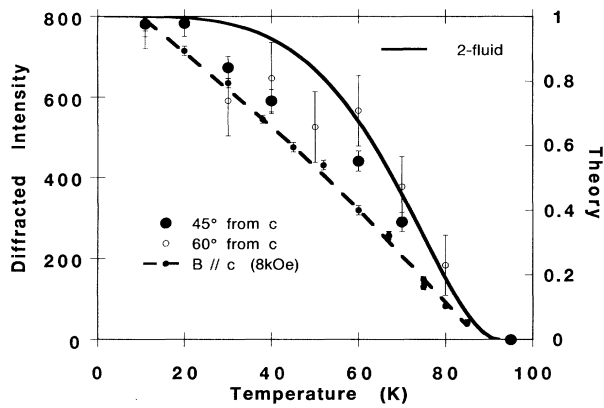


FIG. 5. The temperature dependence of the diffracted intensity for $\Theta=45^\circ$ and $\Theta=60^\circ$ is shown along with the two-fluid expression (solid line) and the data for $\Theta=0^\circ$. (The intensity plotted is averaged over the elliptical ring of spots to improve statistics since individual spots do not appear to have different temperature dependences.) All measurements were made at an applied field of 8 kOe.

well oxygenated sample.

The observed temperature dependence of the intensity is shown in Fig. 5. As is apparent, the main deviation between the measured T dependence and conventional theories is at low temperatures where the intensity begins to fall immediately as the temperature is raised. There appears to be no extended plateau where the intensity has saturated (as seen in the two-fluid curve for $T \approx T_c/3$). However, the intensity drop for the anisotropic lattice is slower than for the $B \parallel c$ data at the same applied field (shown by the dashed line in Fig. 5), where the intensity fell much more precipitously. The dependence for 0

$< T < 50$ K can be estimated adequately by a straight line; however, it is not possible to extract an analytical form of the temperature dependence of the order parameter from these data.

In summary, we note that we have measured the anisotropic flux lattice in YBCO for angles up to 80° from the c axis. We obtain a value for the mass ratio of 20 ± 2 which is consistent with values in the literature. We also observe a nonconventional temperature dependence of the diffracted intensity.

This work was supported in part by the Division of Materials Sciences, U.S. DOE under Contract No. DE-AC05-84OR21400 with Martin Marietta Energy Systems, Inc.

- [1] S. Senoussi and C. Aguillon, *Europhys. Lett.* **12**, 273 (1990).
- [2] D. E. Farrell *et al.*, *Phys. Rev. Lett.* **64**, 1573 (1990).
- [3] M. Yethiraj, H. A. Mook, G. D. Wignall, R. Cubitt, E. M. Forgan, D. M. Paul, and T. Armstrong, *Phys. Rev. Lett.* **70**, 857 (1993).
- [4] R. Cubitt, E. M. Forgan, D. McK. Paul, S. L. Lee, J. S. Abell, H. A. Mook, and P. Timmins, *Physica (Amsterdam)* **180-181B**, 377 (1992).
- [5] J. Schelten, G. Lippamn, and H. Ullmaier, *J. Low Temp. Phys.* **14**, 213 (1974).
- [6] H. F. Hess, C. A. Murray, and J. V. Waszczak, *Phys. Rev. Lett.* **69**, 2138 (1992).
- [7] L. J. Campbell, M. M. Doria, and V. G. Kogan, *Phys. Rev. B* **38**, 2439 (1988).
- [8] I. V. Grigorieva, L. A. Gurevich, and L. Ya. Vinnikov, *Physica (Amsterdam)* **195C**, 327 (1992).
- [9] W. K. Kwok *et al.*, *Phys. Rev. Lett.* **69**, 3370 (1992).
- [10] B. Janossy, D. Prost, S. Pekker, and L. Fruchter, *Physica (Amsterdam)* **181C**, 51 (1991).